AGU PUBLICATIONS

Geophysical Research Letters

RESEARCH LETTER
10.1002/2014GL062898

Key Points:
- The bipolar seesaw during a D-O cycle is simulated accurately
- SH stadial warming leads NH interstadial warming
- The SH lead is a manifestation of subsurface Atlantic Ocean temperatures

Supporting Information:
- Figures S1–S4

Correspondence to:
G. Vettoretti,
g.vettoretti@utoronto.ca

Citation:
Vettoretti, G., and W. R. Peltier (2015), Interhemispheric air temperature phase relationships in the nonlinear Dansgaard-Oeschger oscillation, *Geophys. Res. Lett.*, *42*, 1180–1189, doi:10.1002/2014GL062898.

Received 17 DEC 2014
Accepted 1 FEB 2015
Accepted article online 3 FEB 2015
Published online 26 FEB 2015

Interhemispheric air temperature phase relationships in the nonlinear Dansgaard-Oeschger oscillation

Guido Vettoretti[1] **and W. Richard Peltier**[1]

[1]Department of Physics, University of Toronto, Toronto, Ontario, Canada

Abstract It has previously been suggested that the Southern Ocean might act as a thermal reservoir in mediating the relationship between the northern and southern hemisphere air temperature signals during a Dansgaard-Oeschger cycle. On the basis of a climate model-based analysis, we demonstrate on the contrary that it is equatorial and subtropical North Atlantic thermocline waters that act so as to integrate and damp the northern hemisphere signal to fix the amplitude and phase of the southern hemisphere counterpart to the more intense North Atlantic component of the oscillation. The dynamics of the Southern Ocean component of the Atlantic meridional overturning circulation are critical in explaining the evolution of the interhemispheric temperature phase relationships. European Project for Ice Coring in Antarctica Dronning Maud Land-inferred air temperature variations are in phase with sea surface temperatures north of the Antarctic sea ice edge, suggesting that it is via a fast atmospheric pathway that this temperature signal is transmitted into the Antarctic ice core record.

1. Introduction

Analyses of ice core-derived climate data from the Greenland and Antarctic ice sheets have led to acceptance of the existence of a bipolar seesaw relationship between climate variability in the northern and southern hemispheres [e.g., *European Project for Ice Coring in Antarctica* (*EPICA*) *Community Members*, 2006]. Millennial scale Dansgaard-Oeschger (D-O) oscillations [*Dansgaard et al.*, 1993] are clearly observed in these high-latitude records of temperature change, and their global scale signature has clearly operated throughout the glacial cycle independent of the amplitude of the individual D-O events [*Blunier and Brook*, 2001].

The notion of the operation of an interhemispheric "bipolar seesaw" in climate variability was described early in the literature [*Crowley*, 1992; *Broecker*, 1998]. *Broecker* [1998] proposed that the temperature rise inferred on the basis of Antarctica ice cores resulted from increased ventilation in the Southern Ocean that was supposed to accompany reductions in North Atlantic Deep Water (NADW) formation. The southern hemisphere gradual warming phase of the D-O oscillation which culminates at the Antarctic Isotope Maximum (AIM) observed in ice cores has consistently been noted to moderately lead the abrupt northern hemisphere component of the temperature response. This has often been taken to imply the absence of northern hemisphere control of the phase relationship between air temperature in the two hemispheres. Model-based and proxy data-based studies of this phase relationship during both the glaciation phase of the last glacial cycle and into the last deglaciation have led to the inference of a wide range of time scales for the interhemispheric coupling of climate variability ranging from near instantaneous to a millennium [e.g., *Charles et al.*, 1996; *Rind et al.*, 2001; *Hinnov et al.*, 2002; *Steig and Alley*, 2002; *Barker et al.*, 2009; *Ganopolski and Roche*, 2009; *Pedro et al.*, 2011; *Banderas et al.*, 2014; *Barker and Diz*, 2014]. Using a freshwater forcing-induced coupled model simulation of a D-O cycle, *Schmittner et al.* [2003] proposed a 400–500 year lead of the Greenland signal compared to those of opposite signs in Antarctica. In *Peltier and Vettoretti* [2014], it was shown that freshwater forcing was not required for the occurrence of the D-O cycle. The fundamental physics underlying the oscillation was rather shown to involve a nonlinear salt oscillation, the action of which accurately reproduced the observed seesaw behavior.

Stocker and Johnsen [2003] suggested that a simple heuristic time series-based model might be employed to interpret the connection between the southern hemisphere and northern hemisphere air temperature variations by invoking the existence of a thermal reservoir in the Southern Ocean, which was suggested to act as a diffusive buffer in interhemispheric coupling. Their idea was that the northern

hemisphere signal is communicated to the southern hemisphere almost instantaneously (they had imagined that this could have been related to Kelvin wave propagation to the south) but that the action of a hypothetical "Southern Ocean thermal reservoir" resulted in an integrated and damped signal in the temperature records observed over Antarctica as compared to that characteristic of the North Atlantic. *Barker et al.* [2009] have more recently attempted to provide evidence that the relationship between the northern hemisphere and southern hemisphere is approximately instantaneous within dating uncertainty (300 years) by analyzing a multiproxy record from a marine sediment core situated in the southeast Atlantic. They noted that marine temperature records in the South Atlantic resemble those in Antarctica with more gradual warming and cooling phases. *Capron et al.* [2010] went on to apply *Stocker and Johnsen*'s [2003] model to records of interhemispheric variability from the entire range of D-O interstadial events (DO2 to DO24) from the last glacial cycle to show that the model reproduces the temporal characteristics of submillennial scale interhemispheric variability.

The issue of the circulation of the glacial ocean clearly has important implications for issues other than interhemispheric temperature coupling during the D-O oscillation, in particular concerning the sequestration of glacial atmospheric CO_2 in the more strongly stratified glacial ocean [*Lund et al.*, 2011; *Adkins*, 2013] or through the reorganization of the ventilated branch of the Southern Ocean associated with glacial sea ice advance [*Stephens and Keeling*, 2000; *Ferrari et al.*, 2014]. A clear signature of Glacial North Atlantic Intermediate Water (GNAIW) in the Southern Ocean basins has been documented from isotopic measurements and magnetic properties measured in deep-sea sedimentary cores [*Lynch-Stieglitz et al.*, 1996; *Kissel et al.*, 2008]. In this study we propose an interpretation of the glacial bipolar seesaw in surface temperature by investigating the connection between Atlantic subsurface temperatures and the upwelling of intermediate and deep water in the ventilated thermocline in the South Atlantic frontal zone.

2. Experimental Design

The simulations of the Dansgaard-Oeschger oscillation phenomenon that will serve as the basis for the analysis of the interhemispheric coupling that underlies the bipolar seesaw effect are those recently described in *Peltier and Vettoretti* [2014] (hereafter PV14). The design of these simulations has been discussed in detail therein and need not be repeated in detail here. These Community Climate System Model version 4 [*Gent et al.*, 2011] $1 \times 1°$-based reconstructions of glacial climate have employed the ICE-6G (VM5a) surface boundary conditions for paleotopography, bathymetry, and land ice cover [*Argus et al.*, 2014; *Vettoretti and Peltier*, 2013; PV14; *Peltier et al.*, 2014] for 21,000 years before present. The geographical extent of the Laurentide ice sheet during the latter third (36 to 31 ka B.P.) of marine isotope stage 3 (MIS3) is estimated to have been close to the extent at Last Glacial Maximum [*Dyke et al.*, 2002].

A low (pelagic) background vertical diapycnal diffusivity profile for ocean vertical mixing was assumed with $\kappa = 0.16\,\mathrm{cm}^2/\mathrm{s}$. The ocean model tracer transport equations employ the isopycnal transport and eddy-induced tracer advection of *Gent and McWilliams* [1990]. The simulation was run for 5000 years and was determined to have reached statistical equilibrium after the first 2000 years of integration based on the average strength of the Atlantic meridional overturning circulation (AMOC) and top of the atmosphere radiation balance (see PV14).

It is important to note that this model does not employ freshwater forcing, as has been the case in other model-based studies employed to simulate the D-O oscillation process. Rather, the temperature variations in our model are the result of a self-sustained nonlinear oscillation of the coupled atmosphere-ocean-sea ice system.

3. Results

3.1. The Bipolar Seesaw in Sea Surface Temperatures

The North Greenland Ice Coring Project (NGRIP) and European Project for Ice Coring in Antarctica (EPICA) Dronning Maud Land (EDML) have produced ice core-derived high-latitude surface temperature records through the last glacial period. Two time series of MIS3 D-O oscillations are presented from the NGRIP and EDML ice core records (Figure 1a) on both a $\delta^{18}O$ [*North Greenland Ice Coring Project* (*NGRIP*) *Members*, 2004; *EPICA Community Members*, 2010] and a surface temperature scale [*Huber et al.*, 2006; *Stenni et al.*, 2010]. The

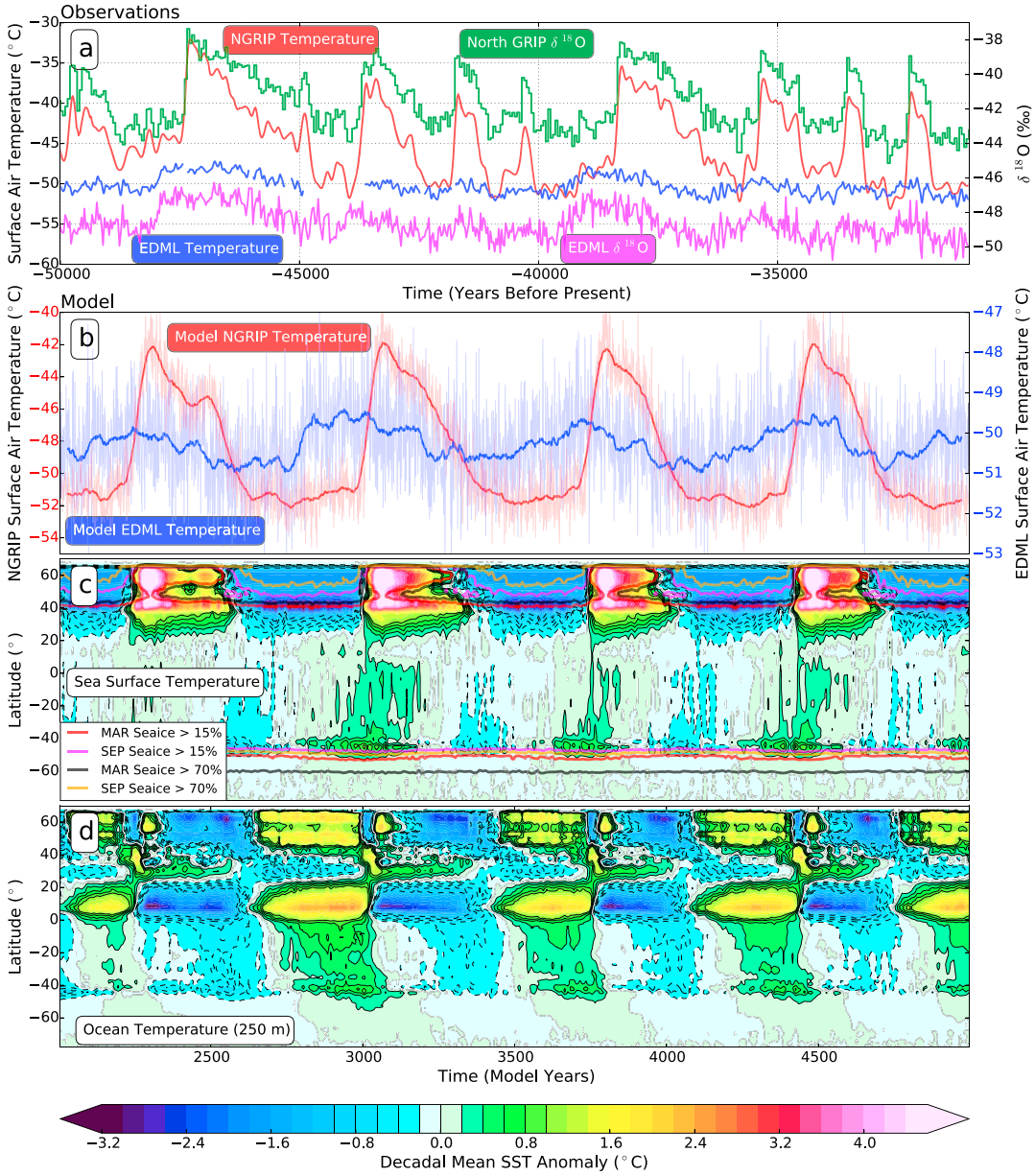

Figure 1. (a) Surface temperature and $\delta^{18}O$ time series from NGRIP [*NGRIP Members*, 2004; *Huber et al.*, 2006] and EDML [*EPICA Community Members*, 2010; *Stenni et al.*, 2010]. (b) Surface temperature time series from the NGRIP and EDML location in the coupled model. (c) Zonally averaged Atlantic SSTs. September and March sea ice >15% and >70% concentration are also contoured. (d) Same as in Figure 1c but for ocean temperatures at 250 m depth.

nature of the AIM in the ice core records reveals that the gradual warming of Antarctic temperature is followed by the rapid onset of the Greenland warming phase of the D-O oscillation, which is nearly coincident with the AIM. Thereafter, the temperature in the North Atlantic gradually decreases in unison with that in Antarctica. The simulated D-O cycles in our model (Figure 1b) provide a realistic representation (in amplitude and phase) of the bipolar seesaw in the NGRIP and EDML records, although the period of the oscillations observed in MIS3 is somewhat longer than those produced by the model. The sensitivity of the predicted period to other parameters of the model will be discussed elsewhere, and PV14 has already demonstrated it to be sensitive to the vertical profile of diapycnal diffusivity.

We further illustrate the nature of the interhemispheric bipolar seesaw by displaying the phase relationship of sea surface temperatures (SSTs) in the model using a Hovmöller diagram of zonally averaged Atlantic SSTs (Figure 1c) and ocean temperature at 250 m (Figure 1d) throughout the coupled model simulation. The South

Atlantic SST maximum just north of the Antarctic maximum (September) sea ice edge leads the North Atlantic SST maximum. Ocean temperatures at 250 m depth (Figure 1d) reveal an almost synchronous temporal correlation between the subsurface temperatures in the North Atlantic and the subsurface temperature signal in the South Atlantic but with a slight apparent lag of the South Atlantic behind the temperatures at this depth in the North Atlantic. The temperature signal does appear to propagate from the north to the south at subsurface and northward at the surface. The southward propagation of the subsurface temperature anomaly is addressed below.

3.2. Atlantic Ocean Circulation

Meridional heat transport between the tropics and the polar regions operates through both atmospheric and oceanic pathways, with one component increasing heat transport to compensate for the other through the action of Bjerknes compensation [*Bjerknes*, 1964; *Shaffrey and Sutton*, 2006] (see Figure S1 in the supporting information). A reduction in cross equatorial ocean heat transport during the "off" (stadial) phase of NADW production has been documented in a number of idealized simulations [e.g., *Manabe and Stouffer*, 1988]. The southward migration of the Intertropical Convergence Zone and corresponding shifts in the Hadley circulation during stadial phases of glacial climate are expected to impact cross equatorial transport of both heat and moisture [*Wunsch*, 2005; *Broccoli et al.*, 2006; *Donohoe et al.*, 2013]. The reorganization of atmospheric transports is also expected to impact the bipolar seesaw to some extent. Here we argue, however, that the dominant changes in SSTs in the South Atlantic are the direct result of the interaction of the Southern Ocean wind-driven upwelling, the AMOC, and diffusive upwelling at low latitudes [*Marshall and Speer*, 2012; *Talley*, 2013]. The Indian and Pacific Oceans are also understood to be important in the transport of deep waters and interbasin heat exchange [*Talley*, 2013], but their role in this analysis is neglected as we demonstrate below that the EDML temperature signal is dominated by the southern Atlantic SST response, specifically the maximum anomaly observed at 45°S latitude (Figure 1c).

The Atlantic northward heat transport (NHT) and AMOC in both the stadial and interstadial phases of this simulation remain active throughout the D-O oscillation (Figure 2). The Atlantic NHT (Figure 2a) during the stadial phase of the D-O oscillation is reduced by approximately half of the interstadial value. During the interstadial, the latitudinal increase in NHT to approximately 30°N indicates that the Atlantic is absorbing heat from the atmosphere and subsequently releasing it to the atmosphere at higher latitudes north of 30°N. In the stadial, the NHT latitudinal maximum is much broader but still implies that the Atlantic is absorbing heat over a large section of the tropical and subtropical ocean. The AMOC stream function for volume transport (Figures 2b–2d) demonstrates that the AMOC maximum increases from approximately 12 sverdrup (Sv) to approximately 30 Sv between the stadial and interstadial states and shoals by approximately 500 m under stadial conditions. During the stadial, the AMOC is characterized by transport of GNAIW southward between approximately 1000 and 2000 m depth [*Lynch-Stieglitz et al.*, 1996]. The shallow meridional wind-driven circulation in the equatorial Atlantic provides a means of southward volume transport south of the equator. An oceanic heat content function can be constructed similar to the meridional stream function for volume transport to diagnose the vertical profile of meridional heat transport in the Atlantic [e.g., *Boccaletti et al.*, 2005; *Greatbatch and Zhai*, 2007]. This diagnostic demonstrates that the modern global surface circulation in the top 500 m south of the equator is responsible for the majority of the global oceanic southward heat transport (see Figure S1 in the supporting information). In the Atlantic, the total heat transport is directed northward even at these southern latitudes. Contributions to southward Atlantic Ocean heat transport result from the north-south transport of NADW and the surface meridional wind-driven circulation (Figures 1c, 2b, and 2c).

During the stadial phase, the AMOC and Antarctic Bottom Water (AABW) cells are separated at an approximate depth of 2000 m in the stream function diagnostic (Figure 2b). This change in the structure of the stratification in the glacial Atlantic Ocean and shoaling of the upper circulation may insulate the bipolar seesaw in temperature from strong vertical mixing. *Ferrari et al.* [2014] propose through a simple theoretical model of the Atlantic Ocean circulation that the southward branch of the shoaled glacial NADW cell becomes isolated from the action of tidally induced mixing as a result of southern hemisphere glacial sea ice advance. In this simulation, we have implemented a low background vertical diapycnal diffusivity ($\kappa = 0.16\ \mathrm{cm}^2/\mathrm{s}$) independent of depth in the interior ocean, as previously noted. The interior ocean vertical background momentum

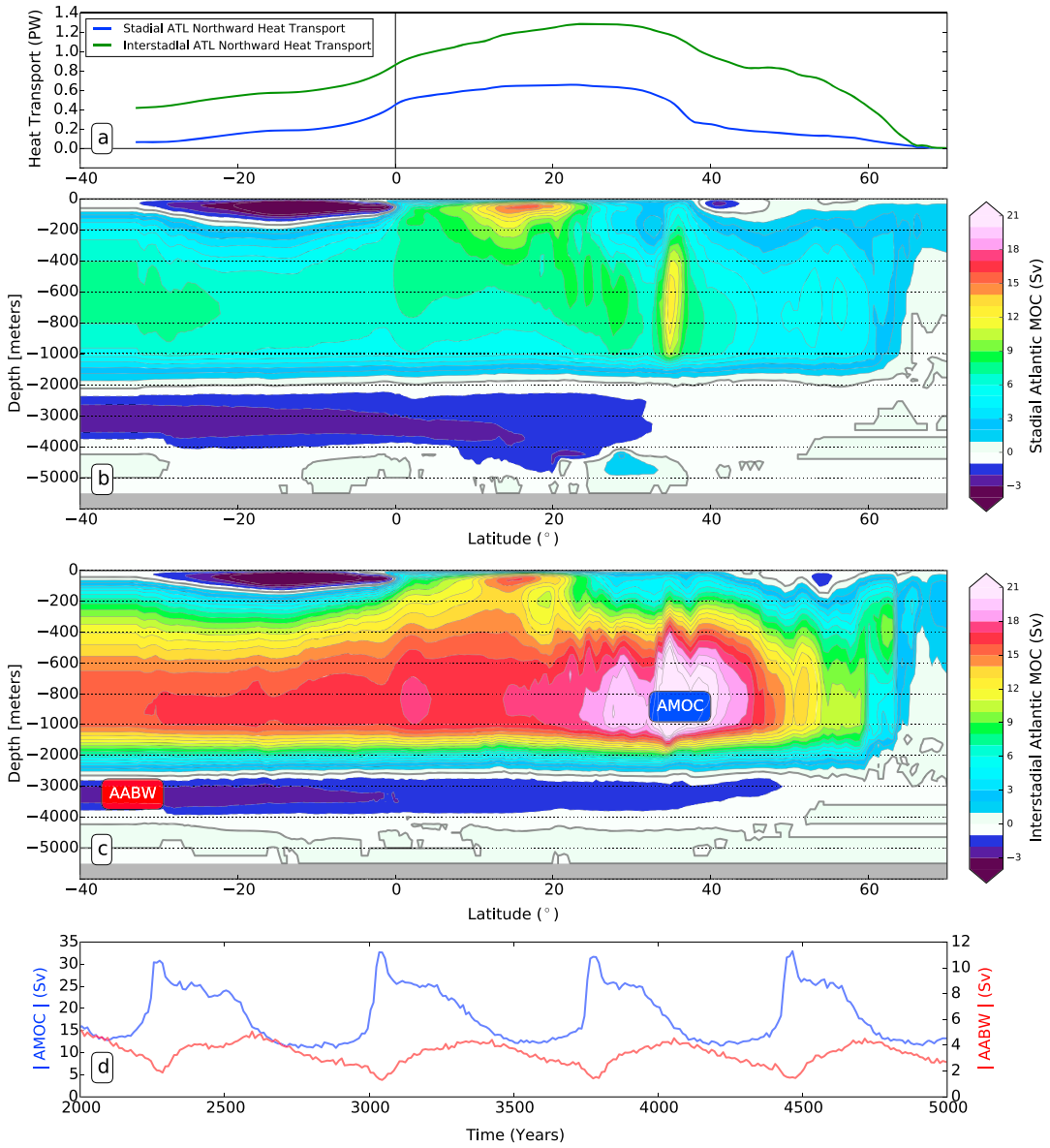

Figure 2. (a) Northward heat transport in the Atlantic basin during the stadial and interstadial phases. (b) Decadal averaged stadial AMOC (at year 2800) and (c) interstadial AMOC (at year 3100) in sverdrup. (d) Time series of the magnitude (sverdrup) of the AMOC and AABW strength are indicated at the locations in Figure 2c.

diffusivity ($\nu = 1.6\,\mathrm{cm}^2/\mathrm{s}$) in the model follows from the assumption that the turbulent Prandtl number has a fixed value of 10 in the model we are employing.

The damped integrated response of the AABW observed in Figure 2d for southern Atlantic overturning may be simply related to a characteristic diffusion time scale associated with vertical momentum transport between GNAIW and the southward return flow of the deeper Atlantic AABW cell. It is clearly evident that at the onset of the rapid increase in NADW formation coincident with the onset of the northern hemisphere warming phase of the D-O cycle, the magnitude of the southern AABW transport begins to increase from its minimum value. The diffusion of momentum from the reinvigorated NADW cell downward into the AABW cell continues even as NADW formation slows during sea ice readvance in the mature portion of the interstadial phase. Increased AABW transport begins to subside when the NADW transport is reduced below modern levels and then further decelerates into the full stadial. The connection between the lower branch of the NADW/GNAIW cell and the upper branch of the AABW cell is physically parameterized in the model as the frictional vertical momentum diffusion associated with the background turbulent eddy viscosity.

Of special note is that the minimum strength of the AABW cell in the Atlantic occurs at precisely the onset of maximum overturning strength of the NADW cell (Figure 2d) as previously discussed in PV14. The temperature signal at EDML in the model (and observations) is approximately 180° out of phase with the strength of the AABW cell (Figures 1b and 2d), meaning that the original suggestion that strengthening NADW production should be accompanied by decreasing AABW production is correct but the southern hemisphere warming signal occurs when AABW production is weak, not when it is strong. The observed and model-predicted correlation is therefore counter to the suggestion of *Broecker* [1998], in which he has suggested that the southern hemisphere warming observed during the stadial phase might be attributed to the activation of AABW formation.

3.3. Interhemispheric Atlantic Subsurface Temperatures

The critical insight required to resolve the interhemispheric puzzle of why the southern hemisphere warming temperature signal leads the northern hemisphere temperature signal follows from an investigation of the evolution of the North Atlantic thermocline temperature and salinity fields during the stadial-interstadial transition. We have previously shown that the D-O oscillation phenomenon is governed by a salt oscillator, in which the salinity gradient between the North Atlantic subtropical gyre and the North Atlantic polar halocline increases in an approximately linear fashion until the onset of the rapid phase of the D-O warming [PV14]. Thereafter, a spike in northward salinity transport ensues as the interstadial AMOC and NHT is reestablished.

An important precursor to the D-O warming instability (Figure 3b) is the establishment of a positive subsurface temperature anomaly in the North Atlantic (NA) below the sea ice-covered stable polar halocline (PH) together with a similarly large subsurface temperature anomaly in the tropics and subtropics, which acts as a thermal reservoir (TR) during the stadial phase in the North Atlantic. These subsurface temperature anomalies (stadial-interstadial) are clearly evident in the meridional and depth-dependent temperature structure of the North Atlantic (Figure 3b). A subsurface warm pool anomaly (~4°C) spans a depth from approximately 150 m to 2000 m in the interval from 40°N to 65°N latitude. Likewise, spanning subtropical latitudes between 30°S and 30°N, a similar subsurface stadial temperature anomaly exists. In the North Atlantic, the establishment of the extremely stable stadial polar halocline allows the ocean vertical column to remain stable (warm below cold) for several hundred years, given the importance of salinity in determining density in the nonlinear equation of state at low temperatures. In the subtropics, we have described above how the system gains heat in the regions where the latitudinal variation of the Atlantic meridional northward heat transport is increasing. The radiative imbalance at the top of the atmosphere is absorbed by the ocean during the stadial phase with a magnitude of approximately 0.5 W/m^2 [PV14]. A fraction of this energy flux goes into establishing the North Atlantic Ocean heat content anomaly during the stadial phase. The existence of this vertical temperature inversion at high latitudes was first suggested by *Rasmussen and Thomsen* [2004], who analyzed planktonic and benthic foraminifera in eight cores in the North Atlantic and Nordic Seas and subsequently invoked the temperature inversion as the main factor involved in destabilizing the water column during the onset of the rapid warming phase of the D-O cycle. This stadial temperature inversion has more recently been further reinforced through high-resolution ocean coring studies [*Dokken et al*., 2013].

Overlain upon the zonally averaged temperature anomaly in Figure 3b are two stadial potential density contours referenced to the surface (σ_0: red contours). The surfaces are plotted to roughly intersect the stadial surface buoyancy flux displayed in Figure 3a. Negative buoyancy flux south of 60°S (related to sea ice brine rejection) in the Southern Ocean matches the March sea ice edge with sea ice concentrations $>$70% (Figure 1c). Thermal buoyancy loss (ocean to atmosphere heat flux) is occurring between approximately 35° S and 45°S. The changes in the sign of the surface buoyancy flux at 60°S can be used to approximately delineate the AABW and NADW/GNAIW water masses ($\sigma_0 = 28.6$ kg/m^3) [*Marshall and Speer*, 2012]. The stadial upper σ_0 surface ($\sigma_0 = 27.1$ kg/m^3) has been plotted to indicate regions of Antarctic Intermediate Water formation. The steeply sloping isopycnals in the Southern Ocean (Figure S2 in the supporting information) are the result of the residual circulation which is derived from a balance between the Eulerian mean wind-driven circulation which acts to steepen the isopycnal slopes and the eddy-induced circulation which acts to reduce the isopycnal slopes through the action of the baroclinic instability process of the Antarctic Circumpolar Current. The isopycnals in the region of the stadial southern Atlantic SST (SS) warm

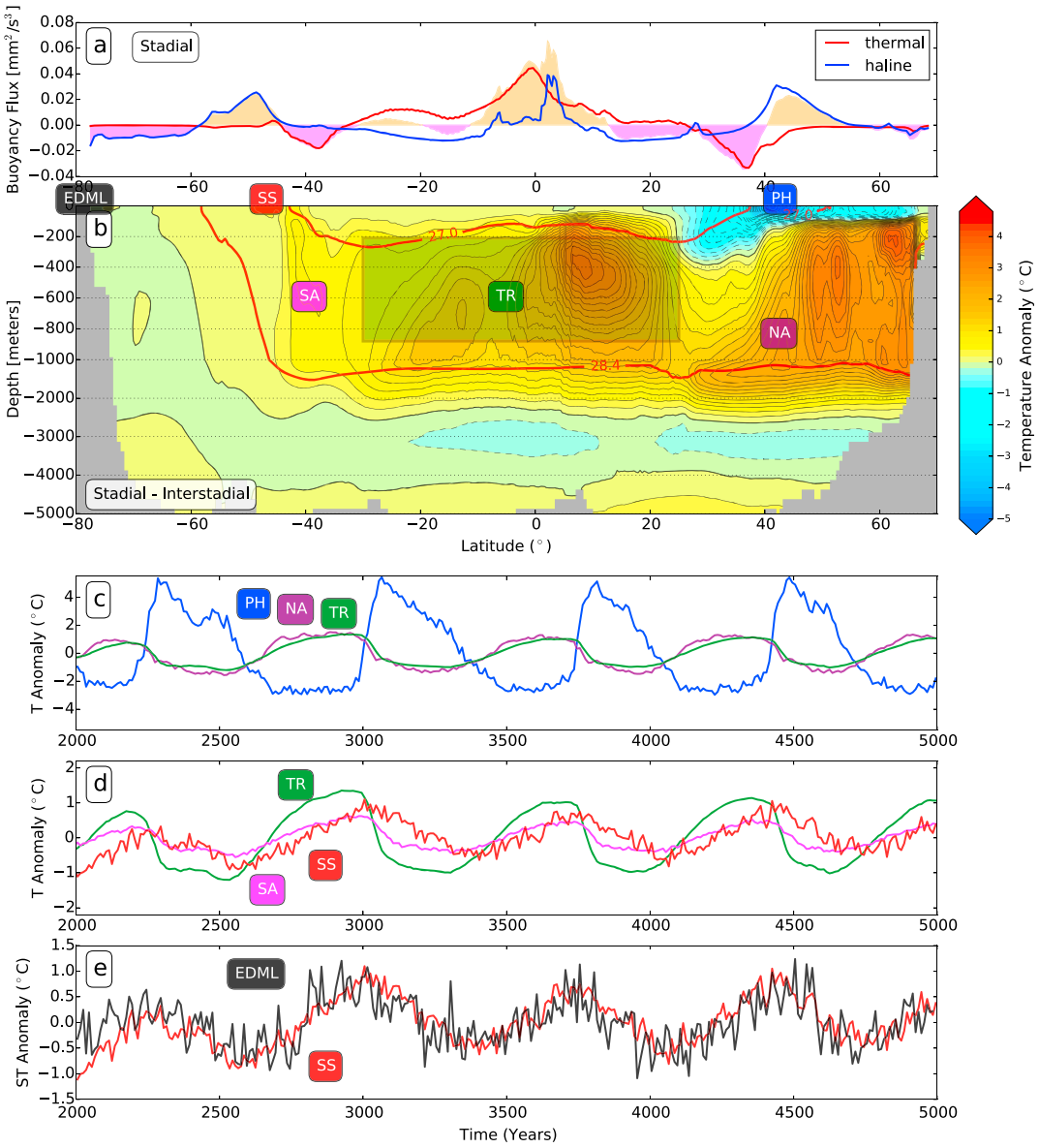

Figure 3. (a) The zonally averaged buoyancy flux over the Atlantic Ocean during the stadial (years 2700–2900). Negative values shaded in pink (positive values shaded in orange) indicate that the ocean surface is losing (gaining) buoyancy on average. The total is the sum of the thermal (red) and the haline (blue) components. (b) Zonally averaged Atlantic Ocean temperatures anomalies (stadial years 2700–2900 minus interstadial years 3100–3300) of a D-O oscillation. Two potential density surfaces (σ_0) from the stadial zonal and temporal Atlantic averages are also shown in red. (c–e) The letters are used for reference locations in the Atlantic plotted as temperature time series anomalies. Anomalies are in reference to a mean state of the four D-O oscillations. PH = polar halocline, NA = North Atlantic, TR = thermal reservoir, SA = South Atlantic, SS = southern mid-Atlantic SSTs, and EDML = EPICA Dronning Maud Land.

anomaly at 45°S (Figure 2b) provide a direct pathway for connection with the deeper South Atlantic (SA) and equatorial thermal reservoirs (TRs).

The release of heat from the central and North Atlantic Ocean heat reservoirs constitute critical aspects of the D-O cycle. During the stadial, the tropical reservoir is delivering a slow and steady input of heat to the southern Atlantic along isopycnals. At the onset of the interstadial, a portion of this tropical/subtropical ocean pycnocline heat reservoir must be released at high northern latitudes as the temperature over Greenland rapidly increases during the onset of the warm phase of the D-O cycle. Even more quickly, the northern reservoir is accessed rapidly as the AMOC reaches maximum amplitude during the onset of the rapid warming component of the D-O cycle [PV14]. Just after the onset of the rapid warming during the interstadial, the

reinvigoration of the AMOC results in tropical/subtropical subsurface temperatures that are anomalously cool. This central Atlantic thermal reservoir is depleted during the interstadial, and therefore, southern Atlantic temperatures reflect these changes in a damped and integrated fashion along with increased cross equatorial heat transport due to changes in the AMOC and the atmospheric Hadley circulation.

Temperature time series in the Atlantic through the D-O cycle are displayed in Figures 3c and 3d. The evolution of the temperature inversion in the North Atlantic is characterized by warmer temperatures (NA) below cooler temperatures (PH) during stadials compared with the mean state. The inverse occurs during interstadials. The time series of the average temperature in the region of the thermal reservoir (TR) evolves synchronously with the temperatures in the thermocline in North Atlantic midlatitudes (Figure 3c). The evolution of the temperature anomalies in the South Atlantic (SA) midlatitudes are of the same characteristic form as those of the thermal reservoir but are approximately half the amplitude. Therefore, the temperature anomalies in the South Atlantic appear to have been diffusively reduced relative to those at more northward latitudes. Comparing the range of the SST anomaly observed at 45°S latitude (SS), we note the influence of atmospheric forcing on the turbulent mixed layer and that the SSTs are colder during the stadial and warmer during the interstadial as compared with subsurface temperatures. The amplitude of the surface signal is also greater than anywhere in the subsurface surrounding this region. Therefore, we conclude that the signal in the mid-South Atlantic (SS) must have a component that is influenced by the atmosphere (see Figures S3 in the supporting information for atmospheric temperature anomalies).

Of special note is the fact that the temperature response seen in the EDML ice core location in the model can be explained by the response of the temperature signal at the sea ice edge at 45°S. In fact, the signal correlation of Atlantic SSTs with EDML falls off at other latitudes away from this region (Figure S4 in the supporting information). The signal must therefore be connected through a near-instantaneous atmospheric pathway over the Southern Ocean which is covered by sea ice.

4. Conclusions

Dynamical changes in the physical carbon pump have recently been suggested to provide an explanation for the changes in the carbon storage in the deep ocean [e.g., *Ferrari et al.*, 2014]. Recently retrieved ice cores throughout Antarctica are providing high-resolution records of global atmospheric CO_2 in the last glacial cycle (e.g., the West Antarctic Ice Sheet Divide [*Marcott et al.*, 2014], Talos Dome, and EDML [*Bereiter et al.*, 2012]). The availability of this new data set may be interpreted to suggest that the AMOC is influencing the global carbon cycle on the centennial time scale.

In this analysis, we have demonstrated that the interhemispheric phase relationship between inferred atmospheric temperature variations in Antarctica and Greenland do not lend themselves to a simple lead-lag analysis as the D-O nonlinear oscillation is self-sustained. The phase relationship between warming atmospheric conditions in the two hemispheres is simply a manifestation of the connection between Atlantic subsurface thermocline water with the surface of the South Atlantic ventilated thermocline and a secondary influence of an atmospheric teleconnection of opposite phase to that in the thermocline. Therefore, a modified version of the idea of an ocean thermal reservoir through which the northern and southern hemisphere temperature signals are connected [*Stocker and Johnsen*, 2003] does apply to the dynamics of the D-O oscillation. However, we now understand that the instantaneous component of *Stocker and Johnsen*'s [2003] thermal bipolar seesaw (T_N and $-T_N$) is confined mostly to the North Atlantic, while the slow damped integrated response of the Southern Ocean temperature signal results from an Atlantic thermocline reservoir located primarily in the equatorial and north subtropical latitudes.

Our results demonstrate that the warming in the South Atlantic is almost in phase with the temperature anomalies below the North Atlantic polar halocline that is established in the stadial phase of the D-O cycle through the massive expansion of northern hemisphere sea ice [PV14] and reductions in Atlantic Ocean heat transport. We have shown that subsurface heat anomalies in the Atlantic equatorial and midlatitude thermocline are connected with southern Atlantic midlatitude SSTs along density surfaces in the Antarctic frontal zones of the South Atlantic. We have also suggested that glacial AABW production follows a momentum-diffused response to the production of GNAIW/NADW formation during the D-O cycle through the action of a frictional momentum coupling between the upper GNAIW/NADW cell and the lower Atlantic AABW cell and that AABW strength is 180° out of phase with the temperatures at Antarctica. We have also

clearly demonstrated that the temperature signal at EDML in the model is essentially perfectly correlated with midlatitude SSTs in the South Atlantic through a direct atmospheric pathway.

Acknowledgments
The research has relied upon computational resources provided by the SciNet facility for high-performance computation of the University of Toronto through the Compute Canada resource allocation process. SciNet is a component of the Compute Canada HPC platform. The research of W.R.P. at Toronto is supported by NSERC Discovery grant A9627. The data employed in the production of this manuscript and supporting information can be provided upon request by contacting Guido Vettoretti, e-mail: g.vettoretti@utoronto.ca.

The Editor thanks Eric Steig and an anonymous reviewer for their assistance in evaluating this paper.

References

Adkins, J. F. (2013), The role of deep ocean circulation in setting glacial climates, *Paleoceanography*, *28*, 1–23, doi:10.1002/palo.20046.
Argus, D. F., W. R. Peltier, R. Drummond, and A. W. Moore (2014), The Antarctica component of postglacial rebound model ICE-6G_C (VM5a) based on GPS positioning, exposure age dating of ice thickness, and relative sea level histories, *Geophys. J. Int.*, *198*(1), 537–563, doi:10.1093/gji/ggu140.
Banderas, R., J. Alvarez-Solas, A. Robinson, and M. Montoya (2014), An interhemispheric mechanism for glacial abrupt climate change, *Clim. Dyn.*, doi:10.1007/s00382-014-2211-8.
Barker, S., and P. Diz (2014), Timing of the descent into the last ice age determined by the bipolar seesaw, *Paleoceanography*, *29*, 489–507, doi:10.1002/2014PA002623.
Barker, S., P. Diz, J. Vautravers, J. Pike, G. Knorr, I. R. Hall, and W. S. Broecker (2009), Interhemispheric Atlantic seesaw response during the last deglaciation, *Nature*, *457*, 1097–1103.
Bereiter, B., D. Lüthi, M. Siegrist, S. Schüpbach, T. F. Stocker, and H. Fischer (2012), Mode changes of millennial CO_2 variability during the last glacial cycle associated with a bipolar marine carbon seesaw, *Proc. Natl. Acad. Sci. U.S.A.*, *109*, 9755–9760, doi:10.1073/pnas.1204069109.
Bjerknes, J. (1964), *Atlantic Air-Sea Interaction*, Advances in Geophysics, vol. 10, pp. 1–82, Academic Press, New York.
Blunier, T., and E. J. Brook (2001), Timing of millennial scale climate change in Antarctica and Greenland during the last glacial period, *Science*, *291*, 109–112, doi:10.1126/science.291.5501.109.
Boccaletti, G., R. Ferrari, A. Adcroft, D. Ferreira, and J. Marshall (2005), The vertical structure of ocean heat transport, *Geophys. Res. Lett.*, *32*, L10603, doi:10.1029/2005GL022474.
Broccoli, A. J., K. A. Dahl, and R. J. Stouffer (2006), Response of the ITCZ to northern hemisphere cooling, *Geophys. Res. Lett.*, *33*, L01702, doi:10.1029/2005GL024546.
Broecker, W. S. (1998), Paleocean circulation during the last deglaciation: A bipolar seesaw?, *Paleoceanography*, *13*(2), 119–121, doi:10.1029/97PA03707.
Capron, E., et al. (2010), Millennial and submillennial scale climatic variations recorded in polar ice cores over the last glacial period, *Clim. Past*, *6*, 345–365, doi:10.5194/cp-6-345-2010.
Charles, C. D., J. Lynch-Stieglitz, U. S. Ninnemann, and R. G. Fairbanks (1996), Climate connections between the hemisphere revealed by deep sea sediment core/ice core correlations, *Earth Planet. Sci. Lett.*, *142*, 19–27, doi:10.1016/0012-821X(96)00083-0.
Crowley, T. J. (1992), North Atlantic Deep Water cools the southern hemisphere, *Paleoceanography*, *7*(4), 489–497, doi:10.1029/92PA01058.
Dansgaard, W., et al. (1993), Evidence for general instability of past climate from a 250 kyr ice-core record, *Nature*, *264*, 218–220, doi:10.1038/364218a0.
Dokken, T. M., K. H. Nisancioglu, C. Li, D. S. Battisti, and C. Kissel (2013), Dansgaard-Oeschger cycles: Interactions between ocean and sea ice intrinsic to the Nordic Seas, *Paleoceanography*, *28*, 491–502, doi:10.1002/palo.20042.
Donohoe, A., J. Marshall, D. Ferriera, and D. McGee (2013), The relationship between ITCZ location and cross-equatorial atmospheric heat transport: From the seasonal cycle to the Last Glacial Maximum, *J. Clim.*, *26*, 3597–3618, doi:10.1175/JCLI-D-12-00467.1.
Dyke, A., J. T. Andrews, P. U. Clark, J. H. England, G. H. Miller, J. Shaw, and J. J. Veillette (2002), The Laurentide and Innuitian ice sheets during the Last Glacial Maximum, *Quat. Sci. Rev.*, *21*, 9–31.
EPICA Community Members (2006), One-to-one coupling of glacial climate variability in Greenland and Antarctica, *Nature*, *444*, 195–198.
EPICA Community Members (2010), Stable oxygen isotopes of ice core EDML, doi:10.1594/PANGAEA.754444
Ferrari, R., M. F. Jansen, J. F. Adkins, A. Burke, A. L. Stewart, and A. F. Thompson (2014), Antarctic sea ice control on ocean circulation in present and glacial climates, *Proc. Natl. Acad. Sci.*, *111*, 8753–8758.
Ganopolski, A., and D. M. Roche (2009), On the nature of lead-lag relationships during glacial-interglacial climate transitions, *Quat. Sci. Rev.*, *28*, 3361–3378, doi:10.1016/j.quascirev.2009.09.019.
Gent, P. R., and J. C. McWilliams (1990), Isopycnal mixing in ocean circulation models, *J. Phys. Oceanogr.*, *20*, 150–155.
Gent, P. R., et al. (2011), The Community Climate System Model version 4, *J. Clim.*, *24*, 4973–4991, doi:10.1175/2011JCLI4083.1.
Greatbatch, R. J., and X. Zhai (2007), The generalized heat function, *Geophys. Res. Lett.*, *34*, L21601, doi:10.1029/2007GL031427.
Hinnov, L. A., M. Schulz, and P. Yiou (2002), Interhemispheric space-time attributes of the Dansgaard-Oeschger oscillations between 100 and 0 ka, *Quat. Sci. Rev.*, *21*(10), 1213–1228.
Huber, C., et al. (2006), Isotope calibrated Greenland temperature record over marine isotope stage 3 and its relation to CH_4, *Earth Planet. Sci. Lett.*, *243*, 504–519.
Kissel, C., C. Laj, A. M. Piotrowski, S. L. Goldstein, and S. R. Hemming (2008), Millennial scale propagation of Atlantic deep waters to the glacial Southern Ocean, *Paleoceanography*, *23*, PA2102, doi:10.1029/2008PA001624.
Lund, D., J. Adkins, and R. Ferrari (2011), Abyssal Atlantic circulation during the Last Glacial Maximum: Constraining the ratio between transport and vertical mixing, *Paleoceanography*, *26*, PA1213, doi:10.1029/2010PA001938.
Lynch-Stieglitz, J., A. van Genn, and R. G. Fairbanks (1996), Interocean exchange of Glacial North Atlantic Intermediate Water: Evidence from subantarctic Cd/Ca and carbon isotope measurements, *Paleoceanography*, *11*, 191–201, doi:10.1029/95PA03772.
Manabe, S., and R. J. Stouffer (1988), Two stable equilibria of a coupled ocean-atmosphere model, *J. Clim.*, *1*, 841–866.
Marcott, S. A., et al. (2014), Centennial scale changes in the global carbon cycle during the last deglaciation, *Nature*, *514*, 616–619, doi:10.1038/nature13799.
Marshall, S., and K. Speer (2012), Closure of the meridional overturning circulation through Southern Ocean upwelling, *Nat. Geosci.*, *5*, 171–180, doi:10.1038/ngeo.139.
North Greenland Ice Core Project Members (2004), High-resolution record of northern hemisphere climate extending into the last interglacial period, *Nature*, *431*, 147–151.
Pedro, J. B., T. D. van Ommen, S. O. Rasmussen, V. I. Morgan, J. Chappellaz, A. D. Moy, V. Masson-Delmotte, and M. Delmotte (2011), The last deglaciation: Timing of the bipolar seesaw, *Clim. Past*, *7*, 671–683, doi:10.5194/cp-7-671-2011.
Peltier, W. R., and G. Vettoretti (2014), Dansgaard-Oeschger oscillations predicted in a comprehensive model of glacial climate: A "kicked" salt oscillator in the Atlantic, *Geophys. Res. Lett.*, *41*, 7306–7313, doi:10.1002/2014GL061413.
Peltier, W. R., D. F. Argus, and R. Drummond (2014), Space geodesy constrains ice-age terminal deglaciation: The global ICE-6G_C (VM5a) model, *J. Geophys. Res. Solid Earth*, *119*, doi:10.1002/2014JB011176, in press.

Rasmussen, T. L., and E. Thomsen (2004), The role of the North Atlantic drift in the millennial time scale glacial climate fluctuations, *Palaeogeogr. Palaeoclimatol. Palaeoecol.*, *210*, 101–116.

Rind, D., P. deMenocal, G. Russell, S. Sheth, D. Collins, G. Schmidt, and J. Teller (2001), Effects of glacial meltwater in the GISS coupled atmosphere ocean model: 1. North Atlantic Deep Water response, *J. Geophys. Res.*, *106*(D21), 27,335–27,353, doi:10.1029/2000JD000070.

Schmittner, A., O. A. Saenko, and A. J. Weaver (2003), Coupling of the hemispheres in observations and simulations of glacial climate change, *Quat. Sci. Rev.*, *22*, 659–671, doi:10.1016/S0277-3791(02)00184-1.

Shaffrey, L., and R. Sutton (2006), Bjerknes compensation and the decadal variability of the energy transports in a coupled climate model, *J. Climate*, *19*, 1167–1181, doi:10.1175/JCLI3652.1.

Steig, E. J., and R. B. Alley (2002), Phase relationships between Antarctic and Greenland climate records, *Ann. Glaciol.*, *35*(1), 451–456, doi:10.3189/172756402781817211.

Stenni, B., et al. (2010), The deuterium excess records of EPICA Dome C and Dronning Maud Land ice cores (East Antarctica), *Quat. Sci. Rev.*, *29*, 146–159.

Stephens, B. B., and R. F. Keeling (2000), The influence of Antarctic sea ice on glacial-interglacial CO_2 variations, *Nature*, *404*, 171–174.

Stocker, T. F., and S. J. Johnsen (2003), A minimum thermodynamic model for the bipolar seesaw, *Paleoceanography*, *18*(4), 1087, doi:10.1029/2003PA000920.

Talley, L. D. (2013), Closure of the global overturning circulation through the Indian, Pacific, and Southern Oceans: Schematics and transports, *Oceanography*, *26*(1), 80–97.

Vettoretti, G., and W. R. Peltier (2013), Last Glacial Maximum ice sheet impacts on North Atlantic climate variability: The importance of the sea ice lid, *Geophys. Res. Lett.*, *40*, 6378–6383, doi:10.1002/2013GL058486.

Wunsch, C. (2005), The total meridional heat flux and its oceanic and atmospheric partition, *J. Clim.*, *18*, 4374–4380.